TWO TRANSPARENT OPTICAL SENSORS FOR THE POSITIONING OF DETECTORS USING A REFERENCE LASER BEAM

J.-Ch. Barrière, H. Blumenfeld, M. Bourdinaud, O. Cloué, C. Guyot, F. Molinié, P. Ponsot, J.-C. Saudemont, J.-P. Schuller, Ph. Schune, S. Sube

CEA Saclay, DSM-DAPNIA, F-91191 Gif sur Yvette Cedex, France

ABSTRACT

We have developed two different optical systems in order to position detectors with respect to a reference laser beam. The first system, a telescope, permits the absolute positioning of an element with respect to a reference laser beam. The resolution is of the order of 10 μm in translation and 50 μrad in rotation. It is highly transparent (~90%) permitting several elements to be aligned. A calibration procedure has also been studied and is currently being tested in order to obtain an absolute alignment information. The second system is a highly transparent (95%) two dimensional position sensor which allows the accurate positioning (below 20 μm) of several (up to ten) elements to which each sensor is attached, transversally to a laser beam used as a reference straight line. The present useful area of the first sensor is 20x20 mm^2 and is 15x15 mm^2 for the second. In both case it can be further increased to meet the experiment's requirement.

1. Introduction

Two new optical sensors have been developed [1] for the alignment of the muon chambers of the ATLAS [2] experiment [(a)]. The momentum measurement in the ATLAS muon spectrometer aims at a precision of the order of 10% for muons of momentum 1 TeV. It proceeds from a sagitta measurement using triplets of precision chambers with a mean distance between chambers of 5 meters. The degree of accuracy needed for the precision chamber alignment is such that the alignment contribution to the final sagitta measurement error stays below the intrinsic chamber measurement error which contributes itself at a level of 50 μm.

For further information -
Ph.S. (correspondence): e-mail: schune@hep.saclay.cea.fr, telephone: (33) 1 6908 7061; fax: (33) 1 6908 6428
J.-Ch.B.: e-mail: barriere@dapnia.cea.fr, O.C.: e-mail: clouc@dapnia.cea.fr, C.G.: e-mail: guyot@hep.saclay.cea.fr,
P.P.: e-mail: ponsot@dapnia.cea.fr, J.-P.S.: e-mail: schuller@hep.saclay.cea.fr

[(a)] ATLAS is an LHC (Large Hadron Collider) experiment, located at CERN (European Laboratory for Particle Physics), CH - 1211 Geneva 23, Switzerland.

In the alignment scheme foreseen for the end-cap chambers [2] , a reference set of 3 to 4 carbon fibre bars are connected by several laser beams. The relative positioning of the bars is done via a laser beam and transparent telescopes precisely mounted on the bars.

The optical alignment sensor useful area should be typically 30x30 mm^2 combined with a transparency above 90% and with a resolution ~10 μm in translation and below 50 μrad in rotation. Up to 180 optical systems with these requirements are foreseen in the end-cap system. An other requirement concerns the price of such a unit which should not exceed • 400.

Finally, the accelerator environment imposes that the system tolerates high particle fluence and dose rates.

In the first part of this paper (sections 2 to 8) we will describe the first sensor, while in sections 9 to 16 the second one is explained. We will compare both in the conclusion (see section 17).

2. Principle of operation of the first optical sensor (STAMP)

2.1 Principle

Our optical telescope, called STAMP for Saclay Telescope for the Alignment of Many Points, allows the accurate positioning of a frame transversally with respect to a laser beam used as a reference or equivalently, provides the laser beam position and direction with respect to a reference frame attached to the sensor.

The laser beam is created by a mono-mode pig-tail diode laser at a wavelength of 680 nm. The chosen wavelength is not critical, but being visible with the eye, the system is easy and safe to operate. The output beam diameter should not exceed 5 mm at distances up to 15 meters (the maximum chamber distance from the laser). Its profile follows a TEM_{00} gaussian distribution. Finally the output power needed must be less than 1mW (see 3.3).

A STAMP is composed of two arms mounted on the same aluminium plate (see Fig. 1 and 2). The first arm consists of a glass window at +45°. This allows to pick up and project a fraction (4%) of the laser beam unto a screen seen by a CCD via a lens operating with a (de)magnification g of the order of 1/10. This magnification is necessary since the range of the displacements is 20 mm (see section 7) and for typical inexpensive CCD the active surface is only ~3x4 mm^2.

The second arm, head to foot with respect to the first one, works on the same principle with the remaining light: another glass window at −45° projects a fraction of the laser beam to a screen, seen with a magnification of 1/10 by a second CCD.

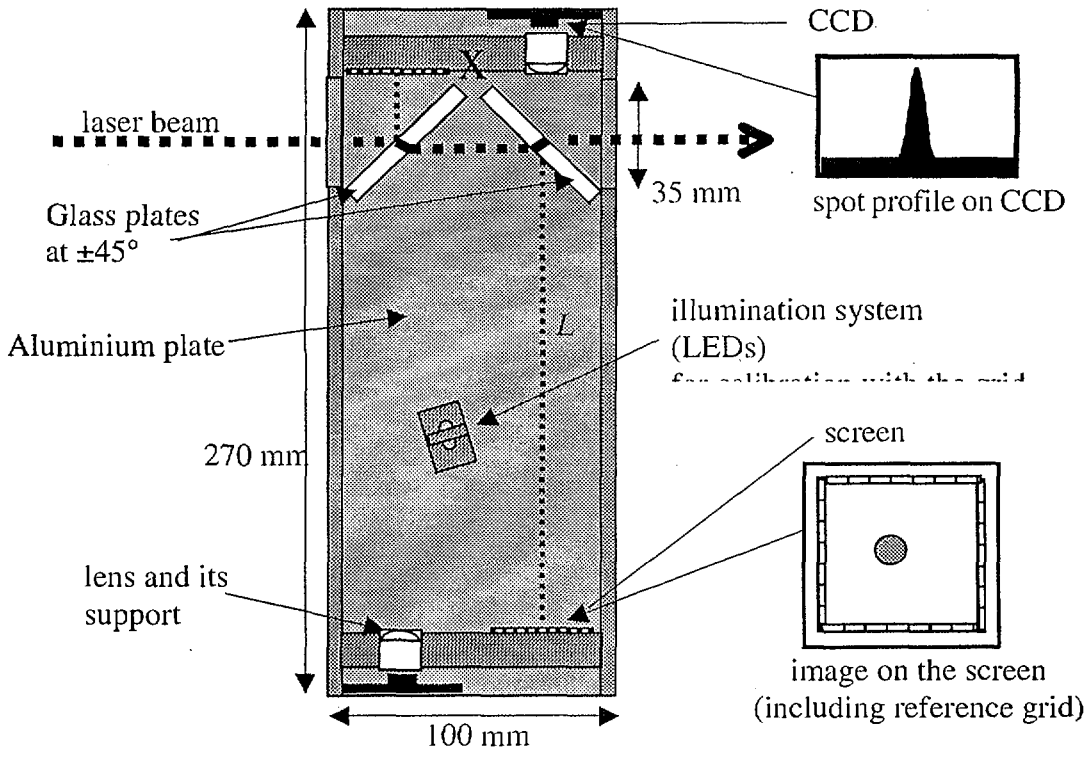

Figure 1 - Sketch of a STAMP showing the two arms. The three-point kinematic mount is located under the aluminium plate (sections 3 and 4). The role of the reference grid is explain in section 4. *L* is approximately equal to the distance between the glass plate and the screen of the long-arm (see text next page).

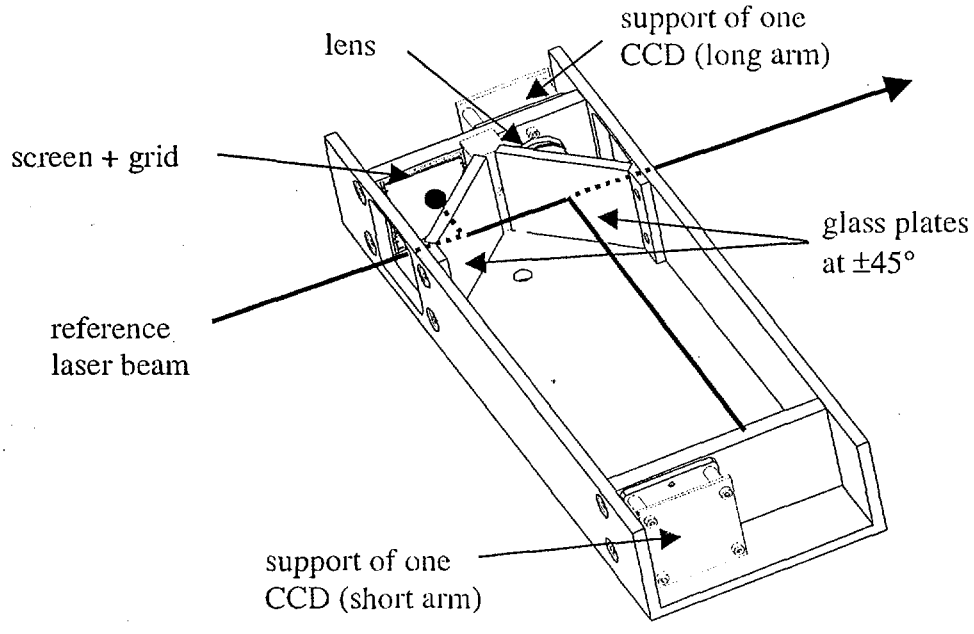

Figure 2 - 3D view of a STAMP. The LED system for the calibration is not shown on this view.

The beam spot on each CCD is recorded and fitted (after the separate summation of all rows and all columns) by a gaussian law for each projection (see Fig. 3).

2.2 Reconstruction of the laser beam position and direction

Using the information from both CCDs allows us to reconstruct the beam with respect to the STAMP transverse position. Assuming a resolution Δd on each CCD, the resolution on the laser spot barycentre is $\Delta d/(\sqrt{2}g)$. The two beam angles with respect to the STAMP reference frame are also accessible to our system because the measurement position from each arm (i.e. the screen position) is different. The angular resolution is simply: $\Delta\theta = \sqrt{2}\Delta d/(gL)$, where L is the distance between the mirror images of the two screens with respect to the reflecting plane of the glass plates (in the present set-up, L is approximately equal to the distance between the glass plate and the screen of the long-arm). With $\Delta d \sim 1$ µm and $g \sim 0.1$ the resolution in translation is below 10 µm. Thus, a distance $L \sim 20$ cm is needed in order to have an angular resolution below 50 µrad.

Thanks to the high transparency of each system (~90%), the positioning of further STAMPs along the same laser beam is possible.

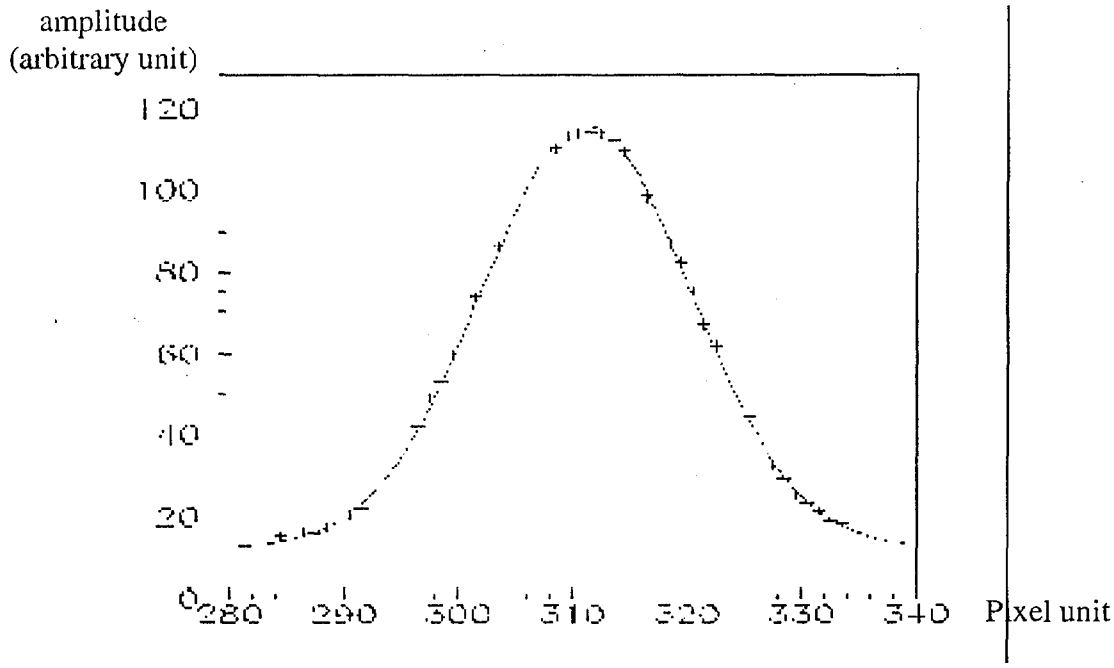

Figure 3 - Example of a laser spot reconstruction (solid line) summing of the pixel rows of the CCD (crosses).

3. Requirements on optical, mechanical and CCD elements

3.1 Optical elements

There are strong requirements on each element in order to reach the expected resolution (<10 μm on each arm) and the required transparency without distortion of the laser beam in case of multiple element alignment.

For high transparency and parasitic image attenuation, an antireflective coating on the exit of the window is optimised for a wavelength of 680 nm. To avoid distortion of the beam, the glass plate must have a flatness tolerance of λ/10 with a wedge angle as small as possible (>1 arc second). Since windows will be used in pairs (one per arm) with angles of ±45°, the angular deflection cancels completely if we can use pairs of windows, cut from a single plate, with the same parallelism. Then the required tolerance is only ~2 arc minutes. Also, if one accept to calibrate the deflection angle, it is possible to relax on these tolerances. Standard surface quality for laser application are required (60–40 scratch and dig or better).

For the lens, the requirements are the following: centration of ~3 arc minutes and a focal length precision of ±2% for the mounting on the system. To avoid a speckle pattern on the CCD, the lens diaphragm diameter is ~ 4 mm for a focal length of 20 mm. A larger aperture may lead to uncontrolled aberrations with a singlet lens.

3.2 Mechanics

To avoid a too big deformation due to temperature variations in the experimental hall (typically ±2°) or during installation, the length of the aluminium plate supporting all the equipment should be as small as possible. Also, the available space in the experiment for each telescope is small. The present overall length of our prototype is about 30 cm and the distance between the screen and the CCD's pixel plane is about 22 cm (this fixed the focal length of the lenses to be 20 mm).

A three-point kinematic mount is used for supporting the plate. The three balls (8 mm diameter) of the support will be used as the reference frame for the absolute calibration (see section 6).

3.3 CCD

For the prototype development phase, we have used video CCDs associated with an 8 bit frame-grabber. With a 1mW pig-tail laser, the laser spot gives up to 200 ADC counts on the CCD, while the dark-current level is about 10 ADC counts. Thus, the contrast is good enough for fitting the spot position with the required precision (~ 1 μm on the CCD).

To avoid interference between the pixel frequency (~9.5 MHz) and the sampling frequency (aliasing) we have used a low-pass Butterworth third order filter. Then, we digitise the signal at ~14.7 MHz, well above the chosen cut-off frequency fc. The latter, $fc \bullet 3$ MHz, is about

one third of the pixel frequency but ten times above the gaussian signal bandwidth in order to avoid phase shift.

4. An optical reference: the grid

4.1 Grid characteristics and function

In order to achieve an absolute positioning (see section 6) and to be independent of the stability of the lens–CCD system, an optical reference has been added on the screen.

This optical reference is made of a photo-lithographic fishbone grid deposited around the 40x40 mm^2 screen (see Fig. 1 and 4). It has a fixed pitch of 1000 µm and a line width of 250 µm. The resolution of the drawing with this technique is better than 0.5 µm.

In standard running conditions, we will alternate laser spot measurement and grid illumination using a LED (for the grid reconstruction algorithm, see 4.2). This grid has several functions:

- the laser spot reconstruction will be done with respect to the grid position independently of the CCD position,
- we can calibrate distortion/aberration of the lens (the grid is regular all around the screen)
- it can be used to calibrate out the imperfect positioning of the optical elements (see Section 6)
- in case of CCD failure, since the screen (including the grid) stays in position, one can replace a CCD without re-calibrating the STAMP.

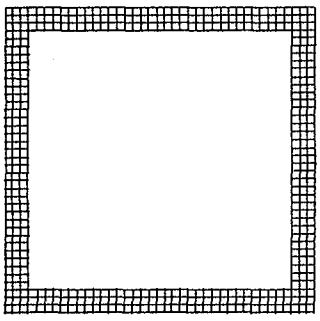

Figure 4 - View of the photo-lithographic fishbone grid deposit all around the screen. The external grid dimensions are about 40x40 mm^2. The useful screen area for the laser spot reconstruction is the inner part of the grid.

4.2 Grid reconstruction on the CCD

We have developed a simple algorithm in order to reconstruct the grid parameters on the CCD. By searching minima along lines and columns of the pixel array, we can reconstruct the grid segments. Combining these segments allows us to determine the crossing points in

horizontal and vertical pixel units. By performing a χ^2 minimisation on all these crossing positions (~300) and using only the grid pitch information, we fit:

i) the magnification g,
ii) the grid position and angle with respect to the CCD axes,
iii) 5 parameters describing the distortion of the lens (9 parameters in total).

To check the consistency of such a fit, we have reconstructed a full square grid (see Fig. 5) on the screen (with the same pitch: 1 mm), fitting these parameters using all the crossing positions or only the border ones. The results are compatible for both fits at a precision level of 3 μm on the screen.

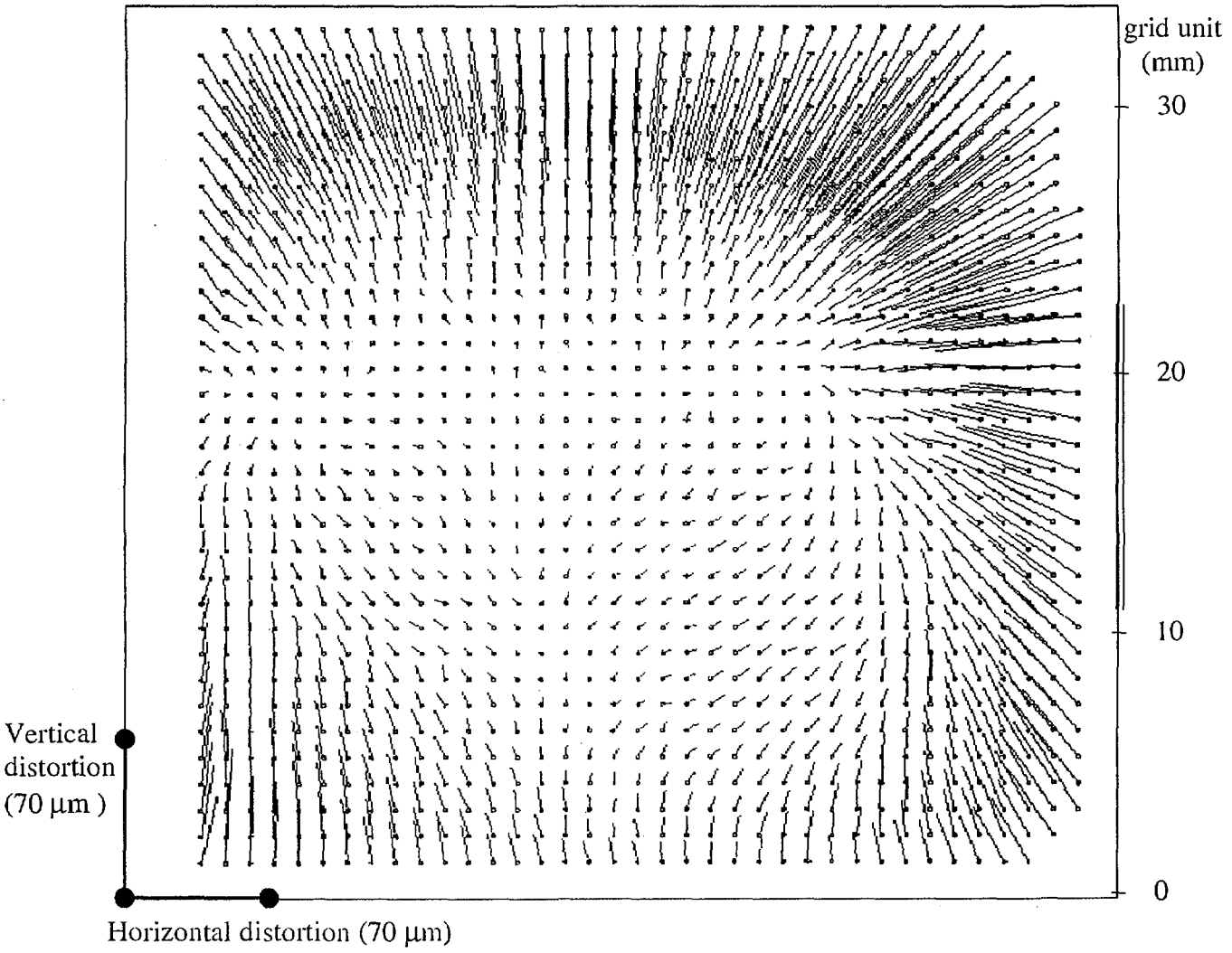

Figure 5 - Calculated distortions, on the screen, using the reconstructed grid on the CCD: the length of each line (horizontally and vertically) gives the amplitude (units on bottom-left scale) of the distortion at each crossing positions (dots; units on right scale). The precision at each crossing positions is better than 3 μm.

5. Experimental set-up and results

5.1 Stability

Every minute, during 24 hours, a laser spot from a pig-tail laser diode has been reconstructed on a STAMP at a distance of 20 cm. In this way, the laser pointing and reconstruction stability can be evaluated: on each CCD, the r.m.s. resolution is below 1% of a pixel, which gives a stability on the screen below 1 μm.

5.2 Resolution when moving the laser

For this test, the laser has been positioned on two perpendicular micro-metric stages. The laser has been displaced in a plane perpendicular to the STAMP at different known positions over a range of ±15 mm. By fitting each reconstructed position on one CCD and by using the laser positions we obtained a resolution on the screen below 10 μm r.m.s. (see Fig. 6). This resolution is corrected for the lens distortion and for the laser's yaw coming from the stages (controlled by an auto-collimator with a resolution of 2 arc-second).

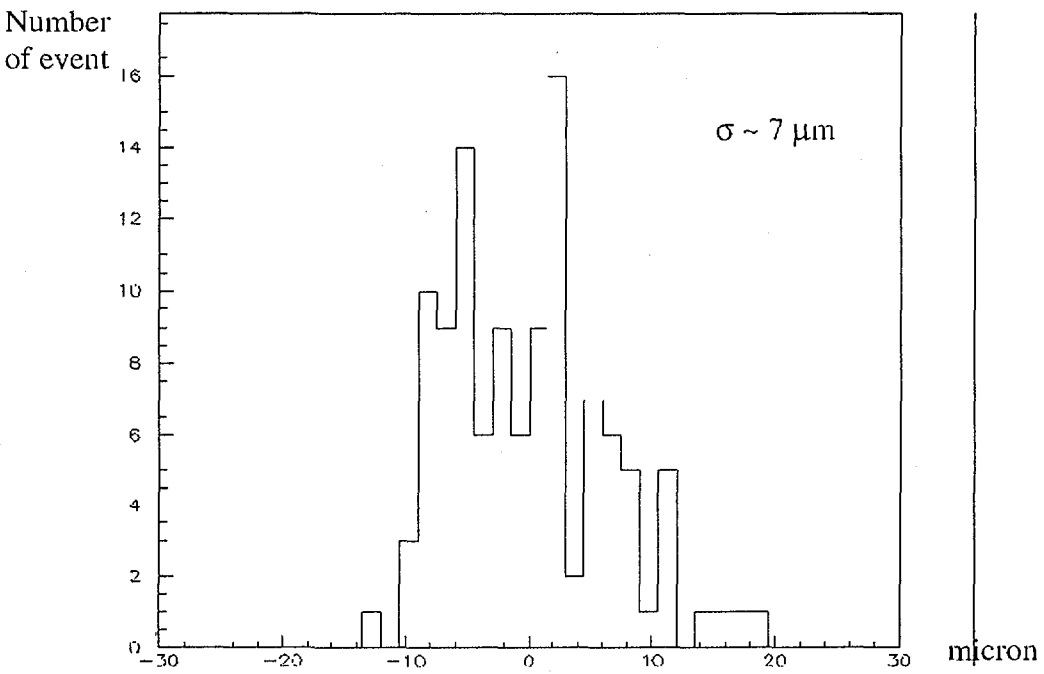

Figure 6 - Reconstructed relative position from one CCD on the STAMP compared to the laser positions from the two perpendicular micro-metric stages. The r.m.s. resolution is 7 μm.

5.3 Question of several STAMPs

A test bench consisting of three STAMPs (see Fig. 7) has been used for testing the influence on the spot deflection due to the displacement of one STAMP with respect to the following one. The first STAMP is fixed and controls the laser pointing stability during the acquisition. The middle one which is moveable deflects the laser due to the induced rotation of its two glass windows. Its relative position is measured by six mechanical probes with a resolution below 2 μm. The last STAMP is fixed and measures the deflection of the laser beam coming from the middle one. The distance between two STAMP is 1 meter.

We have compared the displacements of the middle STAMP over a range of ±4 mm and ±20 mrad, measured by the mechanical probes and by the STAMP itself. For translations the resolution is below 3 μm r.m.s. and for rotations the resolution is below 20 μrad r.m.s. .

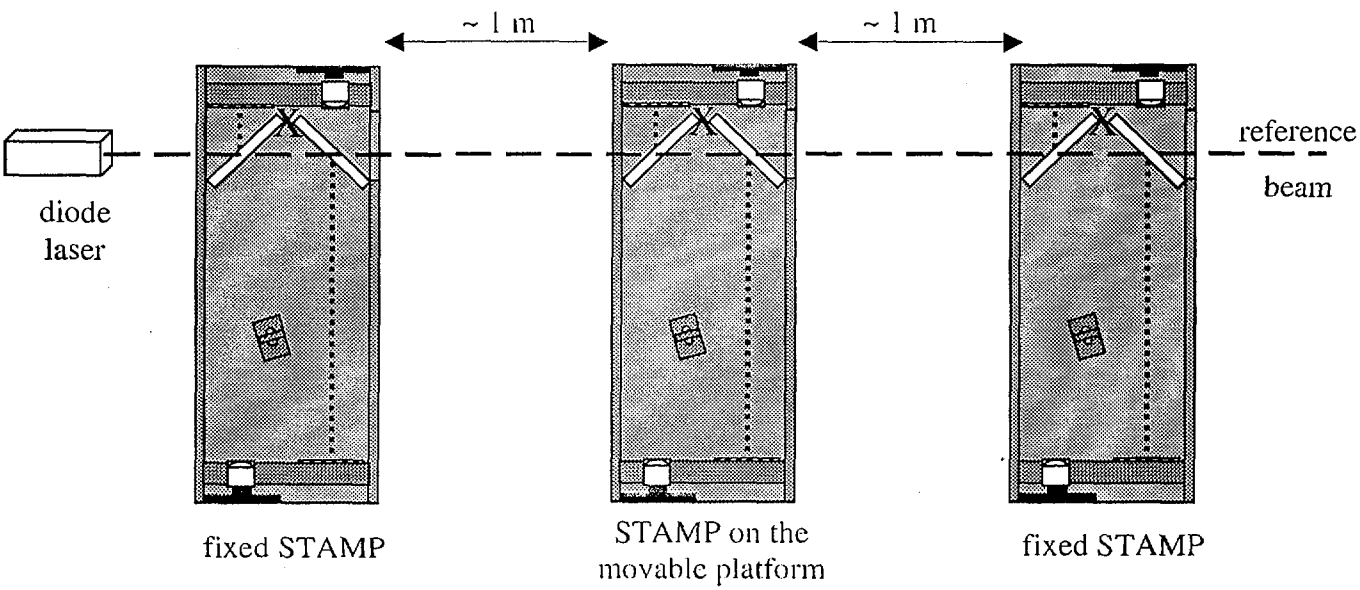

Figure 7 - Test bench with the three STAMPs: the first STAMP controls the laser pointing, the middle one is moveable and deflects the laser and the last STAMP measures the deflection of the laser beam coming from the middle one.

The laser spot displacement on the last STAMP is measured with a resolution of 4 μm r.m.s. .

6. Absolute alignment procedure

The goal of the absolute alignment procedure is to provide the spot barycentre reconstruction with respect to an external mechanical reference defined by the three balls supporting the STAMP. Again the photo-lithographic grid will be useful.

Fig. 8 shows the set-up for such a calibration. An external CCD alternatively records each grid, illuminated uniformly by an external light source, of a STAMP to be calibrated. A complete photo-lithographic grid precisely fixed on an external support is taken as a reference. This support has known dimensions and its grid is placed alternatively at the two mirror image positions of each STAMP grid. A precision of few microns with respect to the balls supporting the STAMP (not shown) can be reached.

We compare the reconstructed position of each grid of the STAMP with respect to the reference grid placed at the two reference positions (see Fig. 8 for the 2nd reference position). In this way, each sub-system grid/glass window will also be positioned/oriented with respect to the ball bearings supporting the STAMP, with the same precision as the mechanical support.

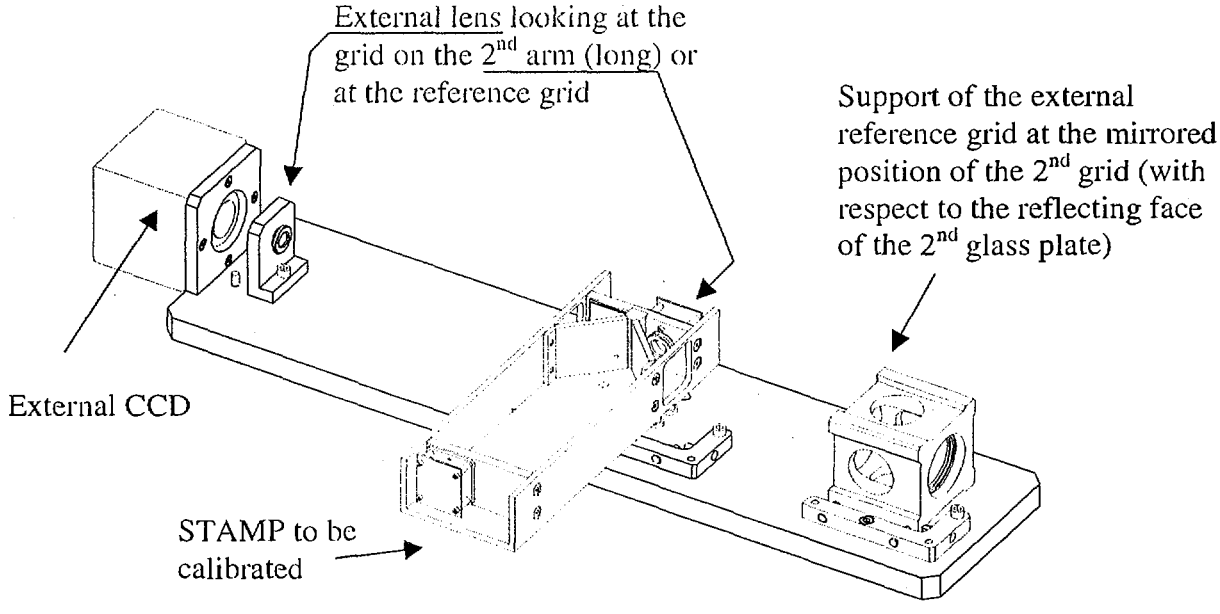

Figure 8 - Set-up for the absolute calibration of a STAMP. The external light sources for illuminating successively the three grids are not shown. The figure corresponds to the reference grid at the second reference position.

This procedure is presently under test at Saclay. Preliminary results indicate that the required precision will be reached.

7. Future tests and development

We plan to use 12 STAMPs in a test bench, simulating a skeleton of an end-cap muon chamber sector, called DATCHA (Demonstration of the ATLAS Chamber Alignment [2]). It will include all other alignment sensors developed for the ATLAS muon chambers [4], for comparison. The temperature inside the experimental hall will be stabilised at ±0.5°.

7.1 Tests to be performed at the DATCHA test bench

For this test, the STAMPs will be associated three by three on the same laser beam (four beams in total) with a mean distance between two STAMPs close to 2.5 m. They will be positioned on carbon fibre bars at known positions, with a relative resolution below 5 μm in all directions. With this set-up the absolute calibration procedure described in Section 6 will be tested. The range of the displacements will be ±10 mm in translation and ±5 mrad in rotation. This is why the present useful area of a STAMP is limited to 20x20 mm^2.

7.2 New CCDs

New CCDs [3] will be used on the DATCHA STAMPs. We have chosen remote driven pixel-CCDs in order to control time exposure, clock speed transfer and real spatial sampling. A special VME electronics board has been designed for this application. It includes multiplexing for several camera readout.

8. STAMP sensor conclusion

We have developed a new type of highly transparent sensor, called STAMP, able to reconstruct a TEM_{00} laser beam profile with a precision of 10 μm in translation and less than 50 μrad in rotation, transverse to the beam. The absolute positioning procedure is currently tested at Saclay using the set-up described in section 6. The range covered by the detector is about 20x20 mm^2. It could be increased without cost implication by enlarging the two screen area and reducing the focal length of the two lenses.

Future studies in real conditions at the ATLAS Saclay-DATCHA test bench will be an important milestone for the absolute calibration procedure including the precise positioning of the detectors on the reference carbon fibre bars (see section 7.1 and [2]).

9. Principle of operation of the second optical sensor (SATRAPS)

The second type of detector which was studied is called SATRAPS for Saclay Transparent Position Sensor. It is made of a square neodymium (1%) doped glass plate, 40 mm to the side and 3 mm thick. The plate faces are flat and parallel (wedge angle <10 μrad). They are

optically polished with a precision of 0.5 μm (λ/2) over a 30x30 mm^2 area. The neodymium is very homogeneous in the glass at a 10^{-6} level ($<10^{-5}$ is required). Fluorescent light, with a wavelength of about 1060 nm (see Fig. 9) produced by a continuous (or pulsed, see section 14) 10 mW laser beam (λ = 680 nm) crossing the plate, is detected by 16 silicon photodiodes (3x10.52 mm^2 each) glued on the edges of the plate (4 photodiodes on each side).

Due to the high transparency of each sensor (> 95%) one can put other SATRAPS (another one in Fig. 9) along the same reference laser beam.

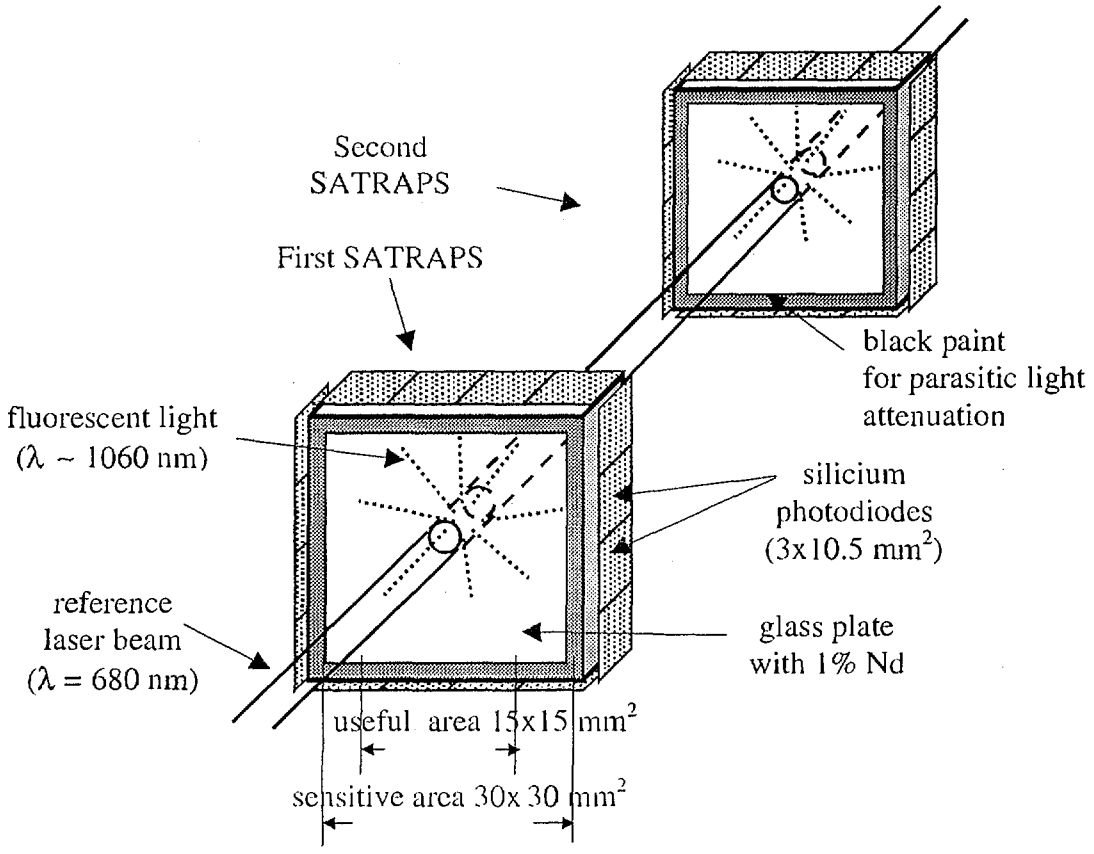

Figure 9 - Two SATRAPS lightened by the reference laser beam. An optic glue connects the photodiodes to the glass plate.

The average position of the optical spot (barycentre) is determined by the relative amount of light detected by each photodiode (see Section 12). Since only 16 photodiodes are combined for the barycentre analysis, a measurement precision of at least 12 bits is required.

10. Electronics

The electronics used to read the photodiode current is located inside a grounded box connected to a PC (Fig. 10). The electronics box is very close to the detector in order to minimise noise affecting the low current intensity (typically 1 μAmp). It contains two cards with the following functions:

a high gain trans-impedance amplifier for current to voltage transformation
a low pass filter for high frequency noise suppression
a low noise gain stage for converter input adjustment
a 16 to 1 channel multiplexer (MUX).

The PC is equipped with an I/O card providing: the multiplexer command for the 16 channels and the multiplexer output signal conversion through a 16 bit A/D converter.

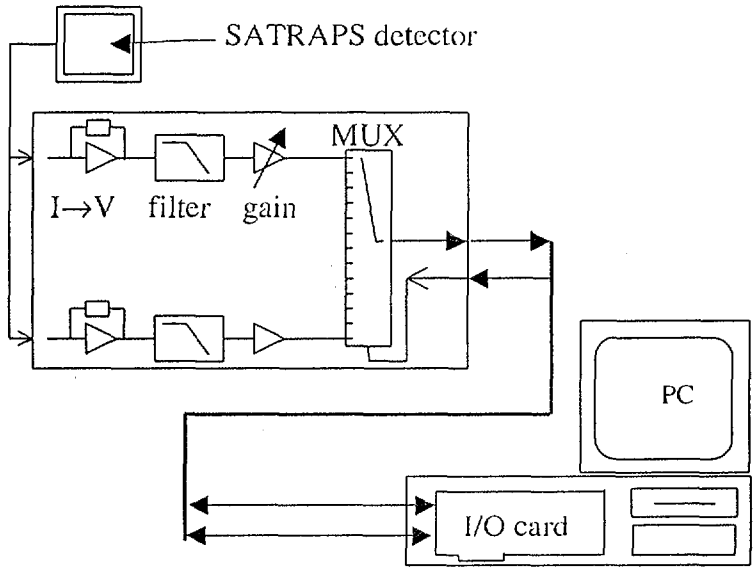

Figure 10 - Electronics readout chain of the photodiodes.

The acquisition takes ~0.5 second for the 16 photodiodes. This delay is dominated by the dialog between the electronics box and the PC I/O card. Finally a software program is used for signal treatment and data formatting.

11. Experimental set-up

In order to evaluate the SATRAPS laser spot positioning precision, we have used the following set-up. A fixed diode laser beam of 1 mm diameter is focused on a SATRAPS, 30 cm away. It can be displaced in a plane transverse to the beam with two micro-metric stages (±1 μm precision) perpendicular to each other (±25 μrad). There are two other SATRAPS in this set-up (see Fig. 11). They are fixed and are used to correct possible time dependent beam pointing variations.

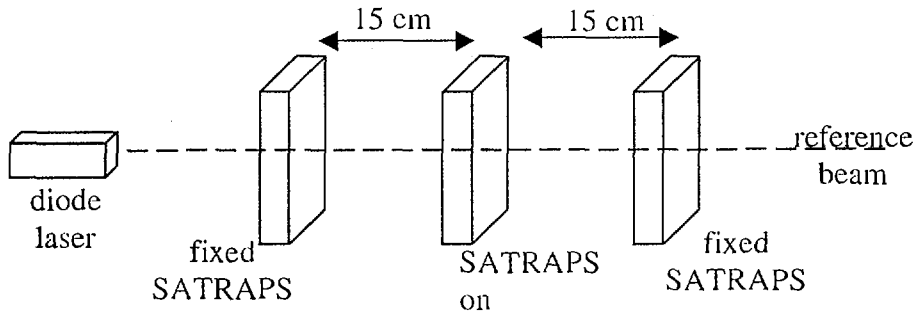

Figure 11 - Experimental set-up.

12. Finding the laser spot position

To determine an unknown laser spot position characterised by the 16 photodiode voltages, a calibration is needed. It is obtained via a reference grid. This grid is built using the illumination of the SATRAPS, by the diode laser, at different precise positions obtained from the micro-metric stages. At each position the 16 photodiode voltages are read out and recorded. The grid has an area of 25x25 mm^2 with a 1 mm step (625 points).

Both horizontal and vertical spot positions are then parameterised each by a polynomial function with 16 parameters. Using these 32 parameters, an unknown spot position can be reconstructed with a 50 μm r.m.s. precision over the entire sensitive area.

A 2-D B-Spline adjustment [5] is performed on each of the 16 photodiode outputs obtained for the 625 grid positions. Then, interpolated points can be used in turn to perform two new more precise 16 parameter fits (for the horizontal and vertical directions). The resolution is around 10 μm r.m.s. (see Fig. 12).

The two other fixed SATRAPS allow for the correction of laser beam pointing instability (after recording a calibration grid for each of them). After these corrections we found the final resolution on the sensor position with respect to the laser beam to be 5 μm r.m.s. .

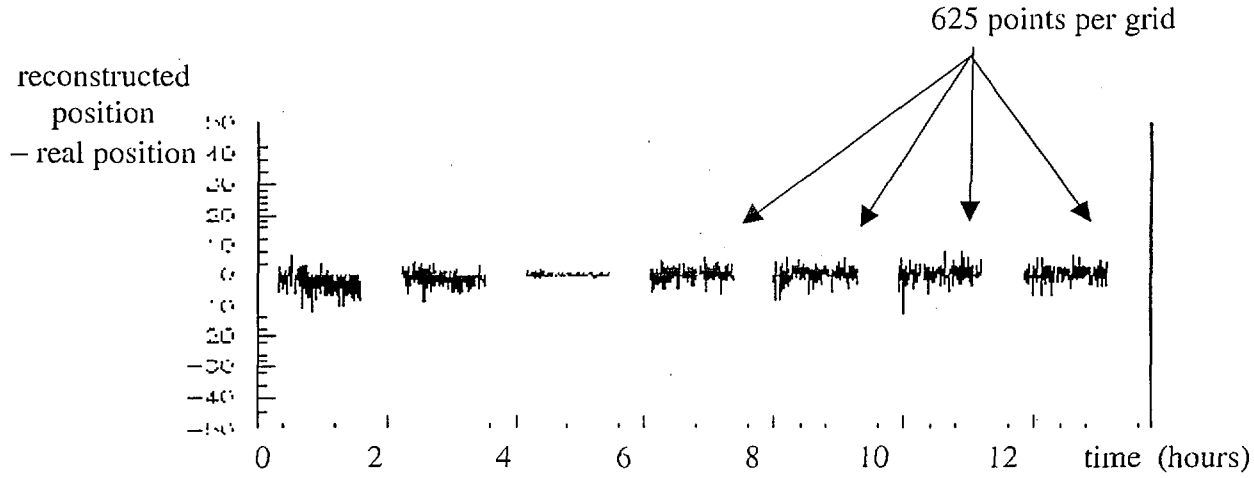

Figure 12 - Resolution as a function of time for 7 successive grids after a 2D B-Spline (see text) has been performed on the *third* grid. Each grid has 625 reconstructed points (it took ~2 hours to be recorded) and is randomly displaced with respect to the *third* grid. Thus, each spot position on grid number 1, 2, 4, 5, 6 and 7 can be considered as unknown spot positions with respect to the calibrated grid (number *3*). The deviation of the spot (of grid 1 and 2) with time can be mainly explained by laser pointing variations (not corrected in this plot) coming from room temperature variations (~1 degree).

A possible solution for the absolute positioning of the laser spot with respect to an external mechanical reference is presented in Section 15.

13. Systematic studies

We have simulated the sensitivity of the resolution to the difference in spot diameter between the calibration position and the measurement position. Indeed a large spot size may induce a different fluorescent light distribution on the photodiodes as compared to a small spot size, thus degrading the final resolution. A Monte-Carlo study has shown that this effect does not increase the resolution by more than 10 μm.

Fig. 13 shows the resolution, for experimental data, when using a laser beam diameter • 1 mm for the fit of the 16 parameters and then applying these parameters to find the spot position for a different laser beam diameter (~ 4 mm). The resolution is ~ 10 μm r.m.s. .

It is important to have a laser spot coming from a pig-tail laser diode in order to have the smallest spot size and to avoid diffuse light all over the plate area even at distances up to 15 m encountered in ATLAS.

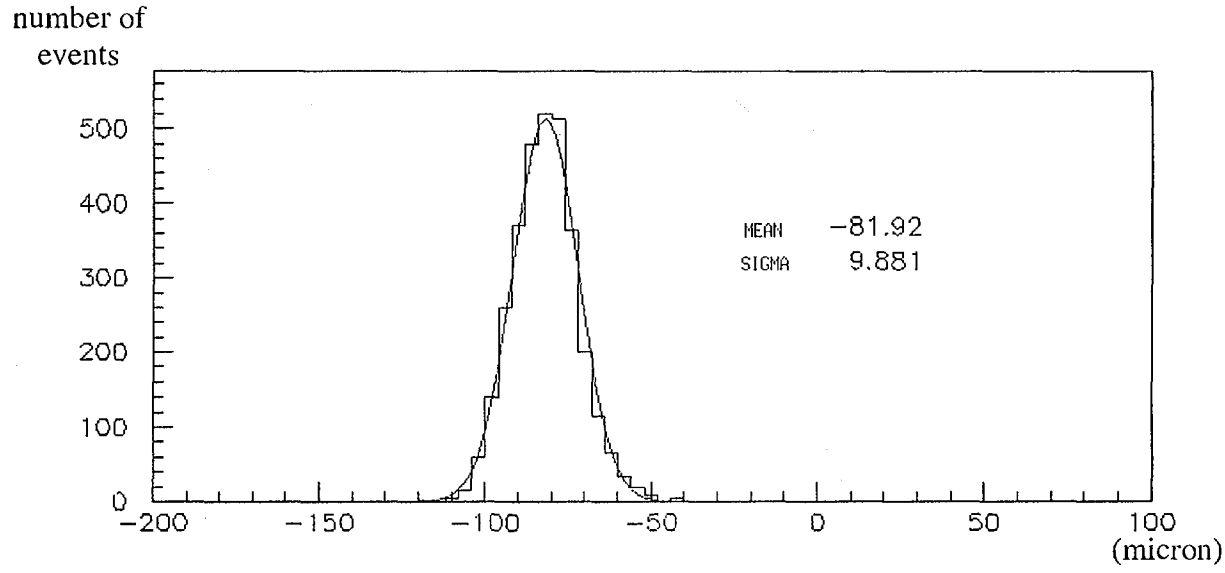

Figure 13 – Difference, in micron, between the reconstructed spot position and the real position given by the micro-metric stages. The reference grid is built with a beam diameter • 1 mm and the ~3000 unknown positions with a beam diameter ~ 4 mm. The mean value (equivalent to an offset in the sensor position) is non-zero since no absolute positioning has been performed for this measurement (see Section 15).

14. Prospects

14.1 Electronics

Some improvement could be made by shortening the data acquisition time in order to eliminate the laser intensity instability which could be at the 1% level. This instability may introduce a systematic shift in the spot centre reconstruction.

The distance between the electronics box and the PC conversion card does not allow fast switching of the photodiode current conversion channels. Also the digital signals made by the I/O board for the acquisition sequence are too slow. Finally, in a system where a large number of detectors have to be measured at the same time, the previous prototype electronics has to be modified.

Considering these aspects new electronics has been designed (Fig. 14). It is located close to the detector and is divided into two boards. The first one performs the 16 photodiode current conversion, the channel multiplexing and the 16 bit A/D conversion. A "Sample and Hold" circuit has been added in front of the multiplexer to avoid laser beam instability problems.

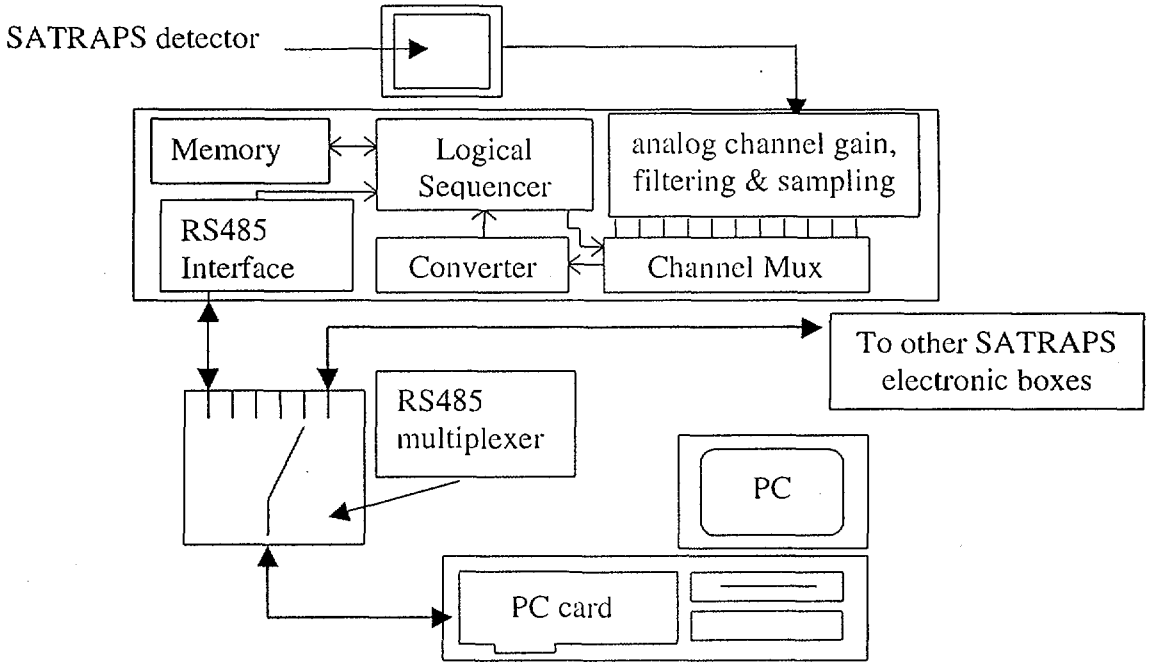

Figure 14 - Possible electronic logic.

The second board contains:

i) the logical sequencer, generating digital signals for channel multiplexing and conversion;
ii) the logical signals for the 16 bit data storage;
iii) the command signals and the data transmission from and to the PC (using a RS-485 protocol).

These two VME size board are placed in a EMI/EMC box which also contains two power supplies.

The RS-485 command line and data transfer signals coming from at least five electronic boxes can be multiplexed within a third board located near the acquisition PC. The expected data acquisition time for one SATRAPS should be less than 1 msec.

14.2 Laser

We considered using a pulsed laser with the electronics describe in section 14.1. Thus, we should synchronise the laser and the electronics. Under these conditions a typical event will consist of at least two measurements (of the 16 photodiodes):

i) one measurement in-between two laser pulses in order to measure the electronics offset and the light background;

ii) one measurement laser on.

A third step may also be useful in-between two laser pulses in order to check the 15 relative electronic gains (see next section 14.3).

14.3 Relative gain control

One can also control (and improve) the stability with time by performing a relative gain measurement of the 16 electronics channels. Indeed, at a 12 bit precision level, the characteristic of some electronic components may vary according to the working temperature, creating a differential gain variation between the 16 channels.

To calibrate the 15 differential gains with respect to one channel (call photodiode number 1 in the following), one can proceed as follows: a LED[(a)] light the sensor through an optical fibre optically glued, therefore fixed, on one corner[(b)] of the doped glass (Fig. 15). In-between to laser pulses and after the offset measurement, we switch on the LED and we record the 16 photodiode currents $c_{i=1,16}$ (another identical system may be added on the opposite corner in order to have enough light on all photodiode with respect to the reference channel –1– . In that case we switch on successively these two LEDs because the relative light from each LED may not be stable at a 12 bit level). The light from the LED should be constant during the record of one event but not necessary identical for all events since the optical fibre is fixed in position.

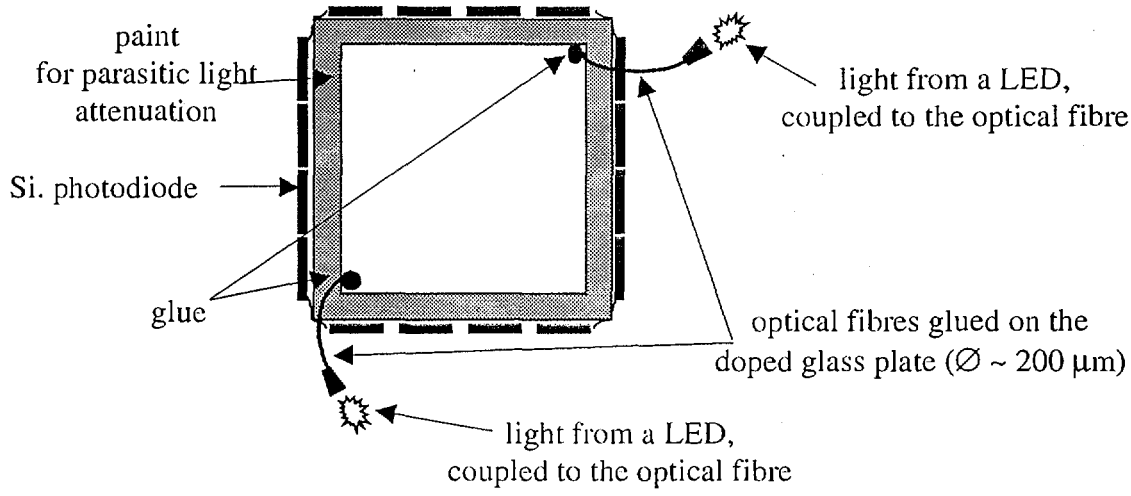

Figure 15 - Measurement of the relative electronic gain with the help of two LEDs, each optically coupled to the doped glass plate through an optical fibre (of course the calibration grid should be done with the two optical fibres in position, see section 12).

(a) The spectral emission of the LED is not necessary centred on the laser wavelength. Indeed, light absorption and thus fluorescent light emission from neodymium is more efficient at wavelength around 580 nm or 740 nm for example.

(b) In this way, the useful area is not affected.

The comparison of the ratio $R^{i,j} = (c_i/c_1)^j$ obtained for event number (j) and $R^{i,k} = (c_i/c_1)^k$ for event number (k), gives for each channel (i) a correction factor $R^{i,j}/R^{i,k}$ which allows to control the relative gain of the 16 channels at a 12 bit precision level (with two LEDs, we take for each channel, the correction factor calculated with the highest current).

15. Absolute spot position

For the previous shown results, each spot mean position was reconstructed with respect to the position of the first spot of the reference grid on the sensor. No absolute position was calculated and this explained the none zero mean value of Fig. 13.

A possible absolute calibration procedure can be performed after the SATRAPS sensor has been fixed on a precise aluminium mechanical support (at right angle).

A photo-lithographic mask on a glass plate is put in front of the active area of the sensor at a distance of ~0.5 mm (see Fig. 16 and 17). This thin mask[(a)] should have a perfect ~300 µm diameter transparent area (called hole in the following) at a known position on that plate. A roundness on the circular area better than 1 µm can be reached. This covering plate and in this way the transparent area, is precisely positioned with respect to the SATRAPS aluminium support. Then, the sensor is lightened only through the hole of the covering glass plate. In order to have a light density as homogenous as possible on the hole we can use a distant laser light perpendicular to the sensor (the required direction precision is <10 mrad). Finally the 16 photo-currents are recorded and the circular area mean position (x_0,y_0) is calculated using the reference grid parameters (see section 12). This reconstructed position is the centre of the circular area [(b)] which is mechanically linked to the support of the sensor. The final precision on the measurement of (x_0,y_0) should be around 10 µm including all mechanical tolerances. After this measurement the covering plate and its support are removed.

After this calibration, each unknown laser spot reconstructed using the reference grid has a calculated position offset (x_0,y_0) with respect to the mechanical support of the optical sensor.

In order to check the validity of this method, we can have 3 or 4 precise transparent circular area on the covering plate each with a known position with respect to the sensor support. The absolute calibration procedure can be reproduce for each hole by lightening them successively. In this way, the offset (x_0,y_0) is measure for each cylindrical hole. Also, we can verify the absolute scale unit on the sensor (which is already fixed by the grid, see section 12) allowing a control of the systematic.

(a) The chrome deposit can be less than 1 µm.

(b) The reconstructed hole position should be independent of the laser position. This is important and it comes from the used of an homogenous lightening of the hole using a diverging laser beam.

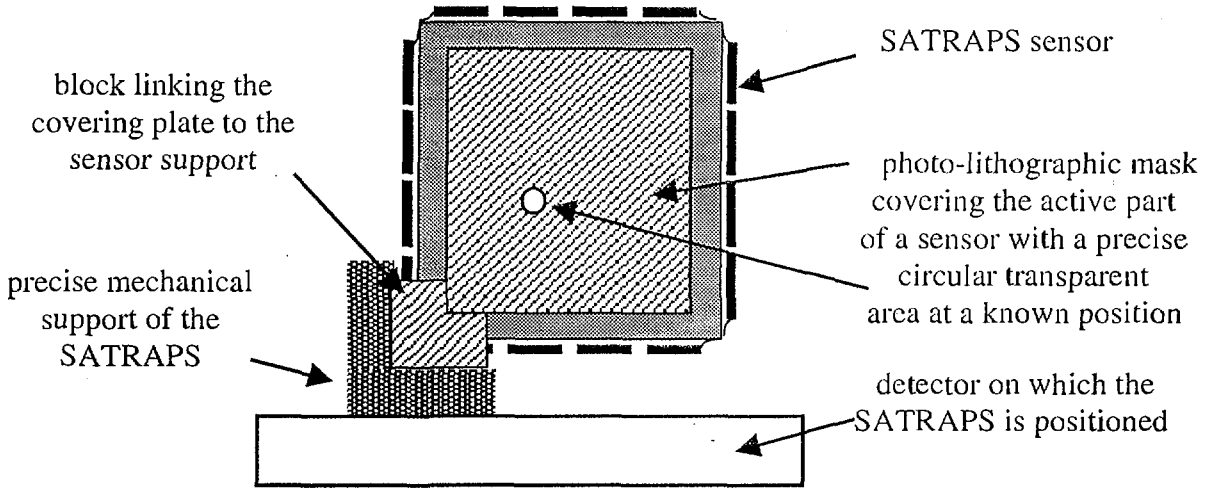

Figure 16 – SATRAPS sensor covered by a photo-lithographic mask with a precise circular transparent area -hole- (front view).

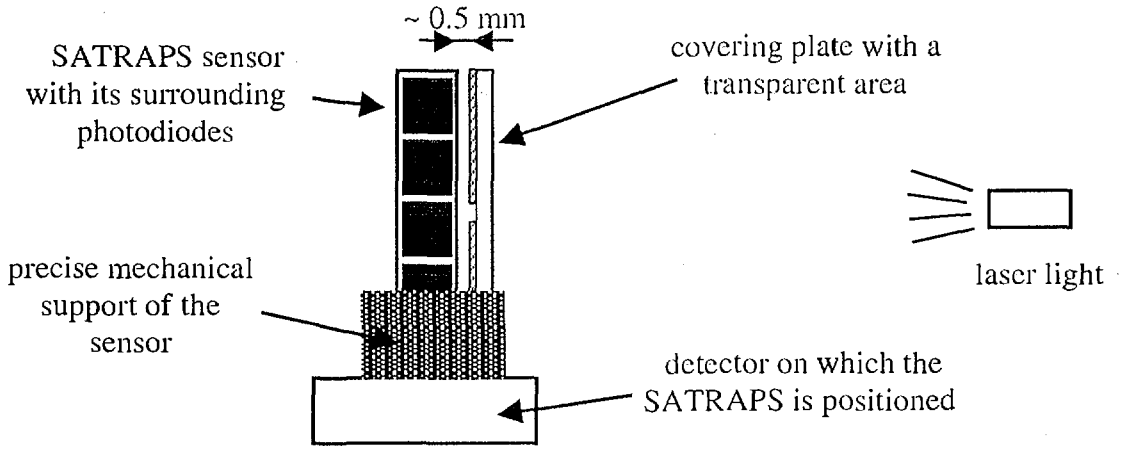

Figure 17 – SATRAPS sensor covered by a photo-lithographic glass plate with a precise circular area -hole- (side view). Here, the reconstructed spot (through the hole) does not depend on the laser position.

16. SATRAPS sensor conclusion

We have developed a new type of highly transparent 2D position sensor, called SATRAPS. For a stable spot size, from a diode laser beam, the typical resolution on a useful area of about 15x15 mm^2 is 10 µm (r.m.s.) using only 16 photodiodes. The resolution is deteriorated

by 10 μm if an unknown laser spot has a different diameter than the one used to built the reference grid. The final resolution is below 20 μm.

A solution to obtain an absolute positioning with respect to an external mechanical reference has been presented. Also, a method to calibrate and control the photodiode relative gain has been described in order to maintain a 12 bit resolution over a long time period.

The size of the doped glass plate of the SATRAPS and thus the useful area could be doubled with the same number of photodiodes without degrading the resolution.

By coupling two SATRAPS on a rigid mechanical support one can build a telescope allowing measurements of translation and rotation, as the first –STAMP– optical sensor described in this paper.

17. Comparison of the two sensors and conclusion

Both sensors are able to locate their position transversally to a reference laser beam. The first sensor (STAMP) has the advantage of an angular measurement and of an absolute positioning which is under test. For this sensor, the resolution transverse to the laser beam is 10 μm in translation and 50 μrad in rotation. The present useful area is about 20x20 mm^2. It has been designed to fulfil the requirements for the future DATCHA test bench, but it can be increased by enlarging the two screen and reducing the focal length of the lens for both arms.

Both sensors operate in the visible which is a great advantage for ease of installation and adjustment and above all from the point of view of safety.

For the second sensor (SATRAPS), the resolution in translation transverse to the laser beam is about 20 μm for a useful area of about 15x15 mm^2. The active area could also be increased by enlarging the sensor area (by a factor of two) with the same number of photodiodes without degrading the resolution. An absolute positioning seems feasible and a possible solution is presented.

For the SATRAPS sensor, the critical component for the radiation tolerance is the optical glue which makes the optical contact between the doped glass plate and the photodiodes. We did not test that component under radiation. The price of such a sensor has not been fully investigated.

For the STAMP sensor the radiation tolerance has been extensively tested for the active components: CCD [6], LED and diode laser.

Finally, all the components used for the STAMP application are well known industrial products, available at a total price already below E 500. It may be reduced further. Twelve

prototypes of this sensor will be tested in a scale one end-cap muon chamber alignment mock-up (the Saclay-DATCHA end-cap project [2]).

18. Acknowledgements

We would like to thank H. v.d. Graaf and K. Hashemi for useful discussions on CCD. We benefited also from the help of the DAPNIA-SIG technical staff.

19. References

[1] "Development of an optical sensor for 2D multi-point alignment", J.-Ch. Barrière et al., NIM-A 387 (1997), 264.
See also: - "Development of a Transparent Optical Telescope for the Absolute Positioning with respect to a Reference Laser Beam", J.-Ch. Barrière et *al.*, Laser Metrology and Inspection, 14-18 June 1999, Munich, Germany. SPIE proceeding, Volume 3823, p. 192.
- "Development of a highly Transparent Fluorescent Optical Sensor for Transverse Positioning of Multiple Elements with respect to a Reference Laser Beam", J.-Ch. Barrière et *al.*, Laser Metrology and Inspection, 14-18 June 1999, Munich, Germany. SPIE proceeding, Volume 3823, p. 212.

[2] ATLAS Technical Proposal, CERN/LHCC/94-43, 15 December 1994,
ATLAS Muon Spectrometer Technical Design Report, CERN/LHCC/97-22, 31 May 1997 and
http://atlasinfo.cern.ch:80/Atlas/Welcome.html.

[3] K. Hashemi and J. Besinger, ATLAS Muon Note 180 (1997).

[4] The ALMY, W. Blum et *al.*, NIM-A 377 (1996) 404.
The Rasnik, H. Groenstege et *al.*, ATLAS Muon Note 63 (1994).

[5] NAG Fortran Library Program, NAG Ltd. Oxford, United Kingdom.

[6] K. Hashemi and J. Besinger, ATLAS Muon Note 253 (1998).